Available online at www.sciencedirect.com
SCIENCE DIRECT®
Chemical Physics Letters 388 (2004) 120–126
CHEMICAL PHYSICS LETTERS
www.elsevier.com/locate/cplett

Femtosecond studies of tryptophan solvation: correlation function and water dynamics at lipid surfaces

Wenyun Lu [a], Jongjoo Kim [a], Weihong Qiu [b], Dongping Zhong [a,*]

[a] Departments of Physics, Chemistry and Biochemistry, The Ohio State University, 174 West 18th Avenue, Columbus, OH 43210, USA
[b] OSU Biophysics, Chemical Physics and Biochemistry Programs, The Ohio State University, 174 West 18th Avenue, Columbus, OH 43210, USA

Received 30 January 2004; in final form 2 March 2004
Published online: 18 March 2004

Abstract

We report here a complete study of solvation dynamics of tryptophan in bulk water with femtosecond resolution and present an accurate method for the construction of its solvation correlation function. The water dynamics was observed in one hundred picosecond (~108 ps) at lipid–water interfaces while in buffer and salt/buffer solutions it becomes faster in tens of picoseconds (~7–20 ps). These water motions are being elucidated on the femtosecond to subnanosecond (or longer) time scale for their different biological functions, such as global structural stability of membranes through well-ordered interfacial water structures and efficient recognition of molecules (and ions) by membrane proteins through ultrafast water displacement.

1. Introduction

The water motions in the hydration layer around a protein surface are central to its structural stability and biological function [1–3]. Various femtosecond-resolved probing strategies have been used to study protein solvation [4–8]. Extrinsic noncovalent labeling of proteins with a dye molecule through hydrophobic interactions usually probes bound-water motions in the crevice of proteins [4–6]. Extrinsic covalent adduction of a dye molecule to proteins probes surface-water molecules but shows limited locations that can be labeled [6,7]. Incorporation of a synthetic fluorescent amino acid into proteins for probing protein electrostatics has been recently reported [8]. Unlike DNA, which can be easily intercalated by a chromophore [9,10] or altered by a base analogy [11], for proteins chemical modification of an intrinsic amino acid residue (cysteine or lysine) is restricted and incorporation of a synthetic one is sophisticated. Direct use of the intrinsic amino acid tryptophan as a local optical probe has been proposed very recently and applied to study protein hydration [12–14]. Ultrafast hydration dynamics (<100 ps) at protein surfaces has been revealed.

Tryptophan has complex absorption and the first two excited singlet states (^1L_a and ^1L_b) are nearly degenerate. They have perpendicular transition moments and the ^1L_a state has a larger static dipole. In polar solvent, the ^1L_a state lies below ^1L_b and the observed fluorescence is dominated from the ^1L_a emission. The photophysics of tryptophan has recently been characterized and the internal conversion of ^1L_b to ^1L_a has been shown to occur ultrafast, in less than 100 fs [12,15]. In the ground state, tryptophan also populates at least two different rotamers. The rotamer dynamics, which is in the range of ~500 ps to several nanoseconds, has been studied extensively [16,17]. Thus, the observed ultrafast solvation dynamics in proteins (<100 ps) is well separated from the internal conversion (<100 fs) and the rotamer dynamics (>500 ps), making tryptophan a powerful optical probe of protein hydration. However, the mixture of two different lifetime emissions makes it difficult to extract solvation dynamics through overall time-resolved spectra of the rotamers.

In this Letter, we report a complete study of tryptophan solvation dynamics in bulk water with femtosecond resolution and present an accurate method to

* Corresponding author. Fax: +1-614-292-7557.
E-mail address: dongping@mps.ohio-state.edu (D. Zhong).

0009-2614/$ - see front matter © 2004 Elsevier B.V. All rights reserved.
doi:10.1016/j.cplett.2004.03.012

construct its solvation correlation function. An important application is given to examine the water dynamics in the lipidic cubic phase (Pn3m) as well as in two common biochemical solutions, a buffer (Tris) and a salt/buffer (NaCl/Hepes) mixture. Different water dynamics ranging from femtosecond to one hundred picoseconds were observed and their biological functions are implied.

2. Experimental

All experimental measurements were carried out by using the femtosecond-resolved fluorescence up-conversion technique. Briefly, the pump pulse is set at 290 nm, doubled from the output (580 nm) of an optical parametric amplifier (OPA) through a mixing of the idler (2109 nm) and the fundamental (800 nm), and the pulse energy was attenuated to 70 nJ. The up-converted signal from 218 to 292 nm was detected by a photomultiplier after passing through a double-grating monochromator. The response time is between 350 and 450 fs as determined from the up-conversion of Raman scattering by water in the range 315–325 nm and from the analysis of the decay time of the up-conversion transient of tryptophan at the blue-side emission (300 nm). Most experiments were done at the magic angle (54.7°) to eliminate the rotational contribution. For anisotropy measurements, the pump beam polarization was set perpendicular ($\perp$) and parallel (//) to the crystal acceptance axis and the resulting femtosecond-resolved transients (I) can be used to construct time-resolved anisotropy: $r(t) = [I_{//} - I_{\perp}]/[I_{//} + 2I_{\perp}]$.

Tryptophan was purchased from Sigma-Aldrich, Tris and Hepes chemicals from USB, lipid monoolein (1-oleoyl-rac-glycerol, >99% purity) from Nu Chek Prep (Elysian, MN), and all other chemical agents from Fisher Scientific. All samples were used as received. The lipid–water mixture was made at 20 °C consisting of 60% (w/w) lipid monoolein and 40% (w/w) water solution which contains 3 mM tryptophan and 20 mM TES buffer at pH 7.4 [18]. This mixture forms the lipidic cubic phase (Pn3m) with a diameter of aqueous channels at ~50 Å [19]. Amphipathic tryptophan preferentially locates at lipid–water interfaces [20], which is also justified by the steady-state emission, time scales of water motions, and femtosecond-resolved anisotropy measurements; see below. The steady-state fluorescence emission of tryptophan in 20 mM TES buffer peaks at 350.5 nm but it shifts to 344 nm in the lipidic cubic phase, indicating a more hydrophobic environment and resembling the emission of a tryptophan residue at protein surfaces [21], while in bulk water the emission peaks at 349 nm. In NaCl (2 M)/Hepes (100 mM) mixture solution (pH 7.5), the emission shifts to the red with a peak at 351.5 nm. In Tris (100 mM) buffer solution (pH 7.5), the peak shifts to 352 nm. For all experiments, samples were kept in various rotating quartz cells to avoid heating and rapid photobleaching.

3. Results and discussion

3.1. Solvation dynamics of tryptophan

The femtosecond-resolved fluorescence transients of tryptophan in bulk water, covering from 300 to 460 nm emission, are shown in Fig. 1. All transients contain two long lifetime emissions (500 ps and 3 ns) [16,17]. At the blue side of the peak emission (349 nm), all transients show decay behaviors with four distinct time scales. For example, at 300 nm emission, the signal decays with time constants of 260 fs (86%), 1.44 ps (11%), 500 ps (2%) and 3 ns (1%). The initial decays at 330 nm increase to 740 fs (35%) and 2.8 ps (11%) with two lifetime contributions of 500 ps (14%) and 3 ns (40%). At the red side of the peak emission, all transients show initial rises with two lifetime emissions. At 380 nm, the signal initially rises in 220 fs (84%) and 1.8 ps (16%) and then decays in

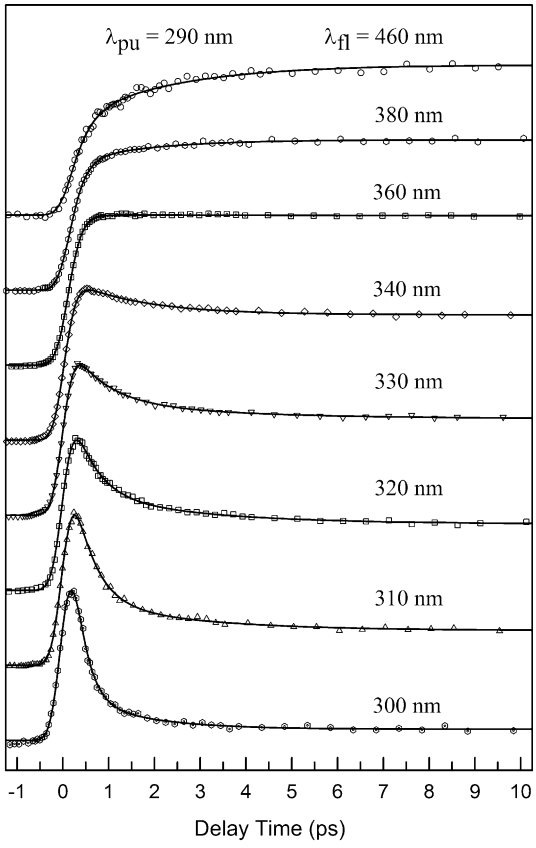

Fig. 1. Normalized, femtosecond-resolved fluorescence transients of tryptophan in bulk water with a series of wavelength detection. Note that the detection was extended to the deep blue side of 300 nm and the far red end of 460 nm.

500 ps (11%) and 3 ns (89%). At the red end of 460 nm, the rises become 320 fs (53%) and 1.85 ps (47%) and the decay is only from the 3-ns contribution (100%). These results are indicative of solvation dynamics and are not due to the electronic relaxation (internal conversion between ^1L_b and ^1L_a) or vibration cooling [12,15].

The solvation dynamics of tryptophan has been recently reported [12,15] and here we extended the fluorescence detection to both the deep blue side (300 nm) and the far red end (460 nm) to obtain a complete study. Larsen et al. [22] recently reported a 16-ps fluorescence decay component at ~460 nm and attributed it to a rotamer dynamics. We did not observe any short-time decay dynamics at the red end for different buffer solutions. Care must be taken to keep tryptophan solution fresh and the sample used for a long time easily gives initial short-time decay at the red end.

3.2. Construction of solvation correlation function

The observed initial femtosecond decay at the blue side and the rise at the red side dominantly result from solvation processes. Typically, by following the standard procedures [23], we can construct the time-resolved emission (Stokes shift with time) and then the correlation function (solvent response curve):

$$c(t) = \frac{\nu(t) - \nu(\infty)}{\nu(0) - \nu(\infty)}, \tag{3.1}$$

where $\nu(t)$, $\nu(0)$, and $\nu(\infty)$ are time-resolved emission maximum in cm^{-1}, respectively. For a molecular probe with only *one* lifetime, $\nu(\infty)$ usually equals to the steady-state emission maximum ν_{ss}. However, tryptophan in the ground state populates at least two rotamers and these excited rotamers in water emit with two different lifetimes (500 ps and 3 ns) and two different emission maxima (ν_1, ν_2). Thus, $\nu(\infty)$ *cannot* be considered to be the apparent ν_{ss}. We need to find out when solvation is completed (t_{sc}) and the corresponding emission maximum (ν_{sc}). In the following, we present a method to determine t_{sc} (and ν_{sc}) from femtosecond-resolved fluorescence measurements.

All femtosecond-resolved transients in Fig. 1 can be best fitted by a sum of a series of exponential functions. These functions can be separated into two parts (assuming no ultrafast quenching of fluorescence emission). One part represents solvation processes and the other one is for lifetime emissions (population decay). The transient signal can be written as follows:

$$\begin{aligned} I_\lambda(t) &= I_\lambda^{\text{solv}}(t) + I_\lambda^{\text{popul}}(t) \\ &= \sum_i a_i e^{-t/\tau_i} + \sum_j b_j e^{-t/\tau_j}, \end{aligned} \tag{3.2}$$

where the first term is for solvation and the second term for lifetime emission. The coefficient a_i is positive (decay dynamics) at the blue side of the emission peak (<349 nm) and is negative (initial rise) at the red side (⩾349 nm). The coefficient b_j is always positive and represents relative contributions of two lifetime emissions (500 ps and 3 ns). The *overall* femtosecond-resolved emission spectra can be constructed as follows:

$$I(\lambda, t) = \frac{I_\lambda^{\text{ss}} I_\lambda(t)}{\sum_i a_i \tau_i + \sum_j b_j \tau_j}, \tag{3.3}$$

where I_λ^{ss} is the steady-state relative emission intensity at λ. For a given t, the emission spectrum can be constructed from the gated transients. The resulting femtosecond-resolved emission spectra of tryptophan in bulk water are shown in Fig. 2a. These spectra are fitted using a log-norm function to deduce the emission maximum $\nu(t)$. Thus, a function of emission maxima with time (ν_s) can be obtained, which is shown in Fig. 2b. At certain time (t_{sc}), solvation is complete and the emission maximum $\nu_s(t_{sc})$ should be equal to the apparent lifetime emission peak $\nu_l(t_{sc})$ (not steady-state peak yet), which results from a mixture of two lifetime emissions and is constructed as follows:

$$I^{\text{popul}}(\lambda, t) = \frac{I_\lambda^{\text{ss}} I_\lambda^{\text{popul}}(t)}{\sum_i a_i \tau_i + \sum_j b_j \tau_j}. \tag{3.4}$$

The lifetime emission maximum function ν_l, also shown in Fig. 2b, merges with ν_s at t_{sc} and the value of ν_{sc} at the merging point could be taken as $\nu(\infty)$ in Eq. (3.1). Thus,

$$c(t) = \frac{\nu_s(t) - \nu_{sc}}{\nu_s(0) - \nu_{sc}}, \tag{3.5}$$

where $c(t)$ stops at t_{sc}. But an accurate way is to subtract the apparent lifetime emission maximum $\nu_l(t)$ from the overall emission maximum $\nu_s(t)$ at any given t and the resulting $c(t)$ is written as follows:

$$c(t) = \frac{\nu_s(t) - \nu_l(t)}{\nu_s(0) - \nu_l(0)}. \tag{3.6}$$

When solvation time is much shorter than the lifetimes, both constructions of $c(t)$ give very similar results because of $\nu_l(t) \approx \nu_{sc}$. However, when solvation dynamics becomes slower, such as in proteins, on a time scale close to the lifetimes, the contribution of $\nu_l(t)$ is significant and Eq. (3.6) must be used to construct $c(t)$. For all results reported here, we used Eq. (3.6). Note that for the molecular probe with only single lifetime emission, $\nu_l(t) = \nu_l(0) = \nu_{ss} = \nu(\infty)$ and Eq. (3.6) becomes to Eq. (3.1).

The key step here is to construct both $\nu_s(t)$ and $\nu_l(t)$ and to determine t_{sc}; see Fig. 2b. When the difference of two maxima ($\nu_s(t) - \nu_l(t)$) reaches 0.5 cm^{-1} we consider solvation complete ($t = t_{sc}$). The difference between ν_{sc} and ν_{ss} purely results from the mixture of two lifetime fluorescence emissions. The time evolution from ν_{sc} to ν_{ss} could be very long. For tryptophan in water, the

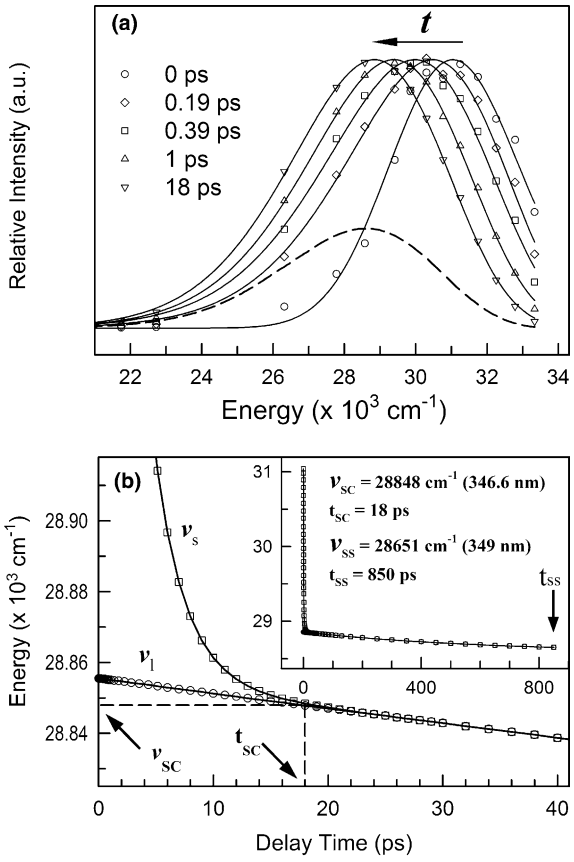

Fig. 2. (a) Normalized, femtosecond-resolved fluorescence emission spectra constructed from femtosecond-resolved fluorescence transients gated at 14 different wavelengths (Fig. 1). The dashed curve is the steady-state emission spectrum peaked at 349 nm. (b) The emission-maximum functions with time constructed from the overall femtosecond-resolved emission spectra in (a), ν_s, and from only two lifetime-emission contributions, ν_l; see text. Note that two functions merge at 28,848 cm^{-1} (346.6 nm) and 18 ps, and solvation dynamics is completed. The spectrum keeps evolution until 850 ps to reach the stead-state emission.

time-zero emission maximum (ν_0) is obtained at 322.1 nm and solvation is completed in 18 ps. Both ν_s and ν_l merge at 346.6 nm and the total Stokes shift is 2186 cm^{-1}. However, it takes another 832 ps for the emission spectrum to reach the steady-state maximum at 349 nm (only 197 cm^{-1} shift due to two emission mixture); see Table 1. In a sense, the steady-state emission maximum is not relevant for construction of the correlation function. The lifetime emission spectrum has a maximum at 329.8 nm for the 500-ps component and at 349.8 nm for the 3-ns component, consistent with previous results [16].

3.3. Water dynamics at lipid–water interfaces and in biochemical solutions

After we understood how to use tryptophan as an optical probe of solvation, we studied the water dynamics at lipid–water interfaces, an important interfacial problem in membrane dynamics, as well as in common salt/buffer solutions. Fig. 3 shows three typical femtosecond-resolved fluorescence transients from more than 10 different gated emissions. Clearly, the interfacial water motions at the lipid bilayer surface drastically slow down. At 300 nm, the transient decays in 0.55 fs (41%), 6 ps (30%), 70 ps (21%) with two long lifetime components (8%). At 330 nm, the initial decays become 1.3 ps (6%), 12.5 ps (15%) and 100 ps (12%). The two lifetime contributions are 67%. At the red side of 440 nm, the transient initially rises in $\sim$ 220 fs (73%), 6.7 ps (12%) and 67 ps (15%) and then decays with two lifetime emissions. In the NaCl (2 M)/Hepes (100 mM) mixture solution, solvation clearly becomes slower than in bulk water. For example, at 330 nm, the transient initially decays in 1.4 ps (35%) and 18.5 ps (8%). The similar results were also obtained in Tris (100 mM) buffer solution (not shown). Using Eqs. (3.3) and (3.4), we constructed femtosecond-resolved emission spectra and the resulting emission-maximum functions of ν_s and ν_l are shown in Fig. 4. As also given in Table 1, the solvation-completed time (t_{sc}) is very different from the time (t_{ss}) for reaching the steady-state maximum. Using Eq. (3.6), all solvation correlation functions probed by tryptophan in different environments are constructed and shown in Fig. 5.

The solvation dynamics of bulk water have been well studied. Jarzeba et al. [24] obtained a correlation function with 160 fs (33%) and 1.2 ps (67%) and Jimemez et al. [25] reported an initial Gaussian-type component (frequency 38.5 ps^{-1} $\approx$25 fs in time width, $\sim$48%), and two exponential decays of 126 fs (20%) and 880 fs (35%). The correlation function we obtained for bulk water is best fitted by double exponential decays integrated with an initial Gaussian-type contribution through a stretched mode: $c(t) = c_1 e^{-(t/\tau_1)^\beta} + c_2 e^{-t/\tau_2}$ where for a pure

Table 1
Emission maxima and times from construction of time-resolved emissions[a]

Tryptophan in/at	ν_0	ν_{sc}	t_{sc}	ν_{ss}	t_{ss}	ν_1	ν_2
Bulk water	322.15	346.64	18	349.0	850	329.75	349.83
Lipid–water interface	321.00	342.40	700	344.1	1100	332.65	346.40
Salt/buffer mixture	322.40	347.44	110	351.5	1200	332.91	352.00
Buffer solution	322.32	348.77	45	352.0	1300	333.37	352.40

See the text for compositions of all mixture solutions.
[a] All emission maxima and times are in units of nm and ps, respectively.

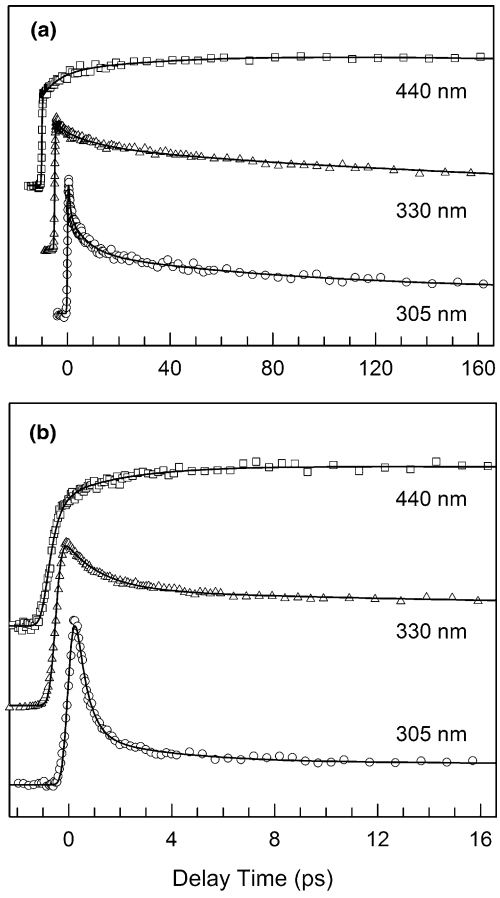

Fig. 3. Normalized, femtosecond-resolved fluorescence transients of tryptophan at the lipid–water interface (a) and in the salt/buffer solution (b) from more than 10 gated fluorescence emissions. Note the different time scales for two panels.

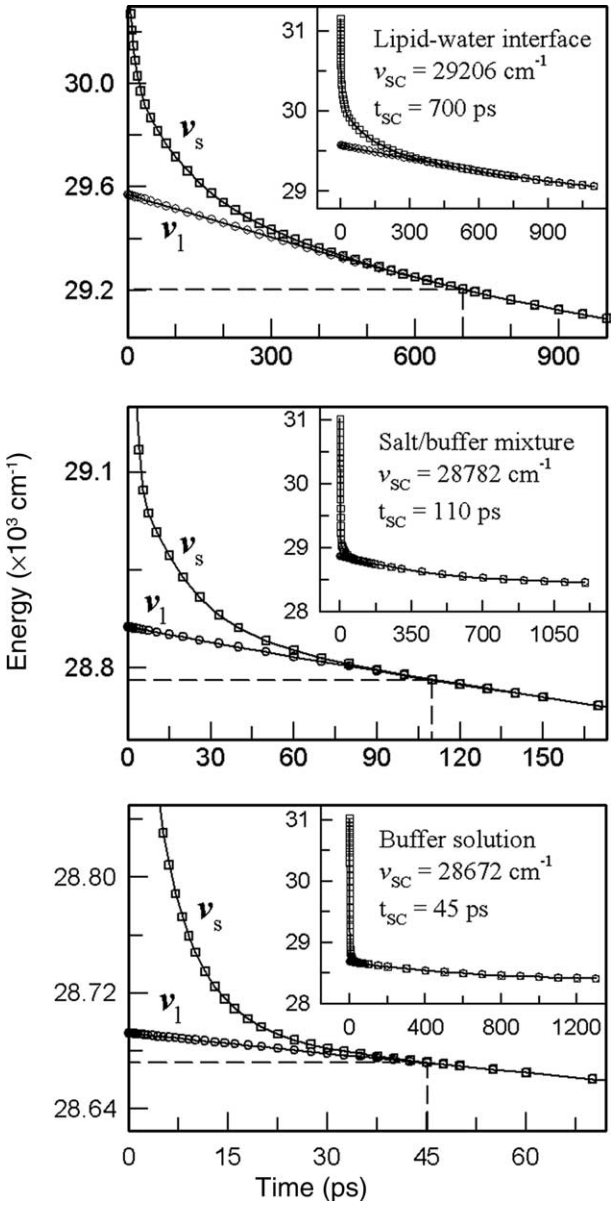

Fig. 4. The emission-maximum functions with time are shown for three different mixtures studied here, which are constructed from the overall femtosecond-resolved emission spectra (ν_s) and from only two lifetime-emission contributions (ν_l); see text. The insets show the entire evolution of ν_s and ν_l. The spectra take longer times to reach the steady-state emissions.

Gaussian-type decay, $\beta = 2$. The final fitting results are listed in Table 2. The 1.6-ps component observed here, which is a little longer than previously reported values (~1 ps), is probably due to the stronger interactions between water molecules and Zwitterionic tryptophan (pH 7.0) in the first solvation shell. For the three biochemical environments studied here, we need to add one more exponential decay term ($c_3 e^{-t/\tau_3}$) to best fit overall correlation function. The results are also listed in Table 2.

The hydration dynamics at the lipid–water interface is drastically slower than in bulk water. The correlation function is modeled by three exponential decays of 560 fs (40%), 9.2 ps (28%) and 108 ps (32%). This observation is striking and indicates well-ordered interfacial water structures. Similar time scales have been observed in lecithin reverse micelles with charged headgroups [26]. For example, when the molar ratio (w_0) of water to the surfactant is less than 4.8 and the mixture is less hydrated, only single exponential decay was observed with a time constant of 219 ps using a dye molecule as an optical probe. While the micelle hydration level increases and w_0 equals to 6.8, triple exponential decay was observed with 570 fs (13%), 14 ps (25%) and 320 ps (62%). It was proposed that the observed three time scales represent three distinct types of water in the micelle, consistent with the original shell model proposed by Finer [27].

According to recent calculations [28], water molecules even at 15–25 Å away from tryptophan could make contributions to tryptophan solvation. The observed hydration dynamics in aqueous channels in the lipidic

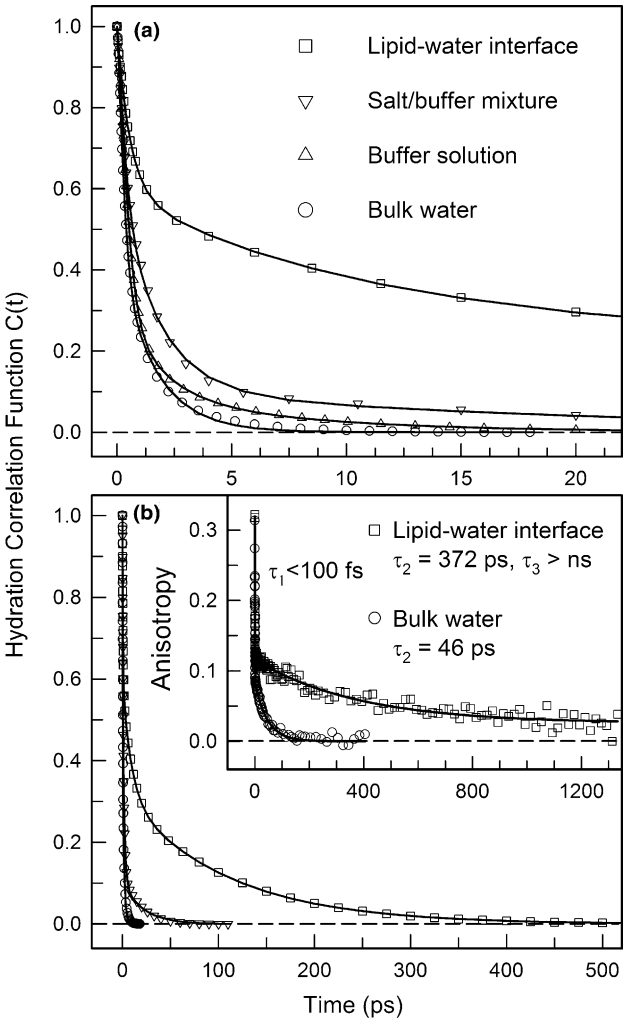

Fig. 5. The hydration correlation functions deduced from Figs. 2 and 4 for four different solutions studied are shown in the short-time range (a) and on the longer time scale (b). For clarity, the long-time water dynamics in the buffer solution is not shown. All these functions are best fitted with multiple exponential decays and the time constants and percentages of each component are given in Table 2. The anisotropy dynamics of tryptophan in bulk water and at lipid–water interfaces are shown in the inset. Note that the anisotropy does not decrease to zero at lipid surfaces, showing that tryptophan anchors at lipid surfaces and experiences restricted local motions.

cubic phase here also supports Finer's model. The 560-fs component represents the bulklike water dynamics around the center of water channels, which is about ~25 Å from the lipid–water interface (the channel diameter is ~50 Å). The 9.2-ps dynamics results from hydrogen-bonding water clusters/networks which are in a dynamic exchange with bulk water (near the channel center) and interfacial water (at the interface). The longest component of 108 ps corresponds to ordered water motions at the interface between the polar headgroups and water molecules, resembling the water dynamics at surfaces of biological membranes. These interfacial water molecules are well orientated and confined in aqueous channels. Water dynamics around the micelle with polar headgroups has been reported with even a longer time scale of 2.44 ns [29]. The lipid chain dynamics was reported to occur on a time scale of longer than nanosecond [30]. A variety of other methods such as vibrational and NMR spectroscopy have been used to interrogate these interfacial water structures [31]. A recent report using a novel coherent anti-Stokes Raman scattering microscopy revealed ordered water molecules between lipid bilayers [32].

The time scale of about 100 ps is ideal for water motions at membrane surfaces. The interfacial water should not be too mobile for global structural stability of lipid bilayers and for unique anchor of membrane proteins. On the other hand, the interfacial water should not be too rigid and the dynamics should be faster than local protein fluctuations (subnanosecond or longer) for efficient recognition and transport of molecules (and ions) through membrane proteins. Thus, hundreds of picoseconds are the actual dynamic time scale of membrane protein–water interactions.

The dynamics of water in salt/buffer and buffer solutions are dominated by bulk water but we observed a long-time decay component in the correlation functions: 7.6 ps in the 100 mM Tris buffer (9%) and 21.4 ps in the salt (2 M)/ Hepes (100 mM) mixture (10%). These times reflect the dynamics of water which is located between tryptophan and the proximate solutes (the buffer molecules or the salt ions). These water motions are one order of magnitude faster than the interfacial ordered-water dynamics and are crucial for ultrafast water displacement and efficient recognition of solutes (ions) by membrane proteins such as in ion channels.

Finally, the femtosecond-resolved anisotropy dynamics, given in the insert of Fig. 5, also indicated the location of tryptophan at interfaces. The initial femtosecond decay (<100 fs) is due to the ultrafast internal conversion between ^1L_b and ^1L_a. The complete orientational relaxation of tryptophan in bulk water takes

Table 2
Results obtained for hydration correlation functions[a]

Tryptophan in/at	τ_1	β	τ_2	τ_3	c_1	c_2	c_3
Bulk water	0.34	1.35	1.6		0.55	0.45	
Lipid–water interface	0.56	1	9.2	108	0.40	0.28	0.32
Salt/buffer mixture	0.41	1.25	1.7	21.4	0.38	0.52	0.10
Buffer solution	0.52	1.35	1.9	7.6	0.68	0.23	0.09

[a] All hydration functions are best fitted with $c(t) = c_1 e^{-(t/\tau_1)^\beta} + c_2 e^{-t/\tau_2} + c_3 e^{-t/\tau_3}$ and $\sum_{i=1}^{3} c_i = 1$. All time constants are in units of picosecond.

~46 ps. If tryptophan is not at the interface, its time-resolved anisotropy would decrease to zero and orientational relaxation would be complete, which is opposite to our observation. The observed time-resolved anisotropy does not decrease to zero and finally stays at a constant of 0.026. The anisotropy due to the orientation relaxation (372 ps) decreases from 0.11 to the final value of 0.026, which reflects restricted local motions [6].

4. Conclusion

In this contribution, we report a complete measurement of femtosecond-resolved fluorescence emission of tryptophan in bulk water and present an accurate method to construct solvation correlation function using tryptophan as an optical probe, which provides a great opportunity for future studies of ultrafast protein dynamics. With this method, we revealed the time scales of water motions at lipid–water interfaces and in buffer and salt/buffer solutions. Understanding of the water dynamics in aqueous channels in the lipidic cubic phase is crucial to membrane protein crystallization. The cubic-phase method has been proposed to crystallize membrane proteins and several examples have been reported [33–35]. However, the molecular mechanism for such crystallization is not yet clear and water is believed to play a central role. The results reported here reveal the actual time scale of lipid–water interactions (~108 ps) and facilitate our further studies of proteins in the lipidic cubic phase.

The time scales of water motions in different biological environments are now clear: 1 ps or less in bulk water; tens of picoseconds around protein surfaces; hundreds of picoseconds at membrane interfaces; nanosecond or longer in protein interiors or crevices (or DNA grooves). Water is so unique and can adopt various structures and have different dynamic motions on a wide range of time scales (fs to ns or longer) for performing different biological functions. The dynamic nature of water in biology (biological water) is now being elucidated at the local atomic scale.

Acknowledgements

This work was supported by the Selective Investment of The Ohio State University through the Biophysics Initiative in the Physics department. We like to thank Prof. Ahmed H. Zewail (Caltech) for many stimulating discussions. Also thanks to Dr. Kenneth Riedl for his preparation of the lipidic cubic-phase sample, Lijuan Wang for her help during experiments and Justin Link for his thorough reading of the manuscript.

References

[1] J.L. Finney, Faraday Discuss. 103 (1996) 1, references therein.
[2] C. Mattos, Trends Biochem. Sci. 27 (2002) 203.
[3] S.K. Pal, J. Peon, B. Bagchi, A.H. Zewail, J. Phys. Chem. B 106 (2002) 12376.
[4] R.R. Riter, M.D. Edington, W.F. Beck, J. Phys. Chem. 100 (1996) 14198.
[5] X.J. Jordanides, M.J. Lang, X. Song, G.R. Fleming, J. Phys. Chem. B 103 (1999) 7995.
[6] D. Zhong, S.K. Pal, A.H. Zewail, ChemPhysChem. 2 (2001) 219.
[7] P. Changenet, C.T. Choma, E.F. Gooding, W.F. DeGrado, R.M. Hochstrasser, J. Phys. Chem. B 104 (2000) 9322.
[8] B.E. Cohen, T.B. McAnaney, E.S. Park, Y.N. Jan, S.G. Boxer, L.Y. Jan, Science 296 (2002) 1700.
[9] E.B. Brauns, M.L. Madaras, R.S. Coleman, C.J. Murphy, M.A. Berg, J. Am. Chem. Soc. 121 (1999) 11644.
[10] S.K. Pal, L. Zhao, A.H. Zewail, Proc. Natl. Acad. Sci. USA 100 (2003) 8113.
[11] S.K. Pal, L. Zhao, T. Xia, A.H. Zewail, Proc. Natl. Acad. Sci. USA 100 (2003) 13746.
[12] D. Zhong, S.K. Pal, D. Zhang, S.I. Chan, A.H. Zewail, Proc. Natl. Acad. Sci. USA 99 (2002) 13.
[13] S.K. Pal, J. Peon, A.H. Zewail, Proc. Natl. Acad. Sci. USA 99 (2002) 1763.
[14] J. Peon, S.K. Pal, A.H. Zewail, Proc. Natl. Acad. Sci. USA 99 (2002) 10964.
[15] X. Shen, J.R. Knutson, J. Phys. Chem. B 105 (2001) 6260.
[16] A.G. Szabo, D.M. Rayner, J. Am. Chem. Soc. 102 (1980) 554.
[17] J.W. Petrich, M.C. Chang, D.B. McDonald, G.R. Fleming, J. Am. Chem. Soc. 105 (1983) 3824.
[18] V. Cherezov, J. Clogston, Y. Misquitta, W. Abdel-Gawad, M. Caffrey, Biophys. J. 83 (2002) 3393.
[19] M. Caffrey, J. Struct. Biol. 142 (2003) 108.
[20] W. Yau, W.C. Wimley, K. Gawrisch, S.H. White, Biochemistry 37 (1998) 14713.
[21] E.A. Burstein, N.S. Vedenkina, M.N. Ivkova, Photochem. Photobiol. 18 (1973) 263.
[22] O.F.A. Larsen, I.H.M. van Stokkum, A. Pandit, R. van Grondelle, H. van Amerongen, J. Phys. Chem. B 107 (2003) 3080.
[23] M. Maroncelli, G.R. Fleming, J. Chem. Phys. 86 (1987) 6221.
[24] W. Jarzeba, G.C. Walker, A.E. Johnson, M. Kahlow, P.F. Barbara, J. Phys. Chem. 92 (1988) 7039.
[25] R. Jimenez, G.R. Fleming, P.V. Kumar, M. Maroncelli, Nature 369 (1994) 471.
[26] D.M. Willard, R.E. Riter, N.E. Levinger, J. Am. Chem. Soc. 120 (1998) 4151.
[27] E.G. Finer, J. Chem. Soc. Faraday Trans. 69 (2) (1973) 1590.
[28] J.T. Vivian, P.R. Callis, Biophys. J. 80 (2001) 2093.
[29] K. Bhattacharyya, Acc. Chem. Res. 36 (2003) 95.
[30] R. Cassol, M.T. Ge, A. Ferrarini, J.H. Freed, J. Phys. Chem. B 101 (1997) 8782.
[31] T. De, A. Maitra, Adv. Colloid Interface Sci. 59 (1995) 95.
[32] J.X. Cheng, S. Pautot, D.A. Weitz, X.S. Xie, Proc. Natl. Acad. Sci. USA 100 (2003) 9826.
[33] E.M. Landau, J.P. Rosenbusch, Proc. Natl. Acad. Sci. USA 93 (1996) 14532.
[34] H. Luecke, B. Schobert, J.K. Lanyi, E.N. Spudich, J.L. Spudich, Science 293 (2001) 1499.
[35] V.I. Gordeliy, J. Labahn, R. Moukhametzianov, R. Efremov, J. Granzin, R. Schlesinger, G. Buldt, T. Savopol, A.J. Scheidig, J.P. Klare, M. Engelhard, Nature 419 (2002) 484.